DRIVING GALACTIC TURBULENCE BY SUPERNOVA EXPLOSIONS

MAARIT J. KORPI

Dept. of Phys. Sci., Astronomy Division, University of Oulu, Finland[1]

A. BRANDENBURG

Dept. of Mathem., University of Newcastle upon Tyne, UK[2]

I. TUOMINEN

Dept. of Phys. Sci., Astronomy Division, University of Oulu, Finland[3]

Summary: *We investigate the general properties of supernova driven interstellar turbulence using local three-dimensional MHD simulations under Galactic conditions. Our model includes the effects of large-scale shear due to Galactic differential rotation, density stratification, compressibility, magnetic fields, heating via supernova explosions and parameterized radiative cooling of the interstellar medium. In addition to investigating isolated supernova explosions we allow for multiple supernovae distributed randomly in the Galactic disc and exponentially in the vertical direction. Single supernova explosions drive a strong shock, the lifetime of which is approximately 2 Myr in our model. This stage is found to be characterized by a kinetic energy spectrum in the diffuse gas with spectral index consistent with* $k = -2$. *Large-scale shear and Coriolis force act on the supernova remnant producing some vorticity inside it, but this process was found to be very weak. In the case of multiple supernova explosions, older remnants have an important role causing density fluctuations in the interstellar medium. In this "clumpy" medium, the propagation velocity of the shock fronts changes due to the changing density, and vorticity is generated. In the absence of these supernova interactions the kinetic energy spectrum shows a relatively wide shock spectrum with spectral index* $k = -2$, *but when the supernova interactions become dominant the classical* $k = -5/3$ *spectrum is observed.*

Key words: Interstellar turbulence, supernova explosions

1. INTRODUCTION

The interstellar medium (ISM) is a highly turbulent flow. Interstellar turbulence, however, is significantly different from the turbulence observed in homogeneous, isotropic and incompressible laboratory flows. The ISM is inhomogeneous, having a multi-phase structure: there are cold dense clouds and hot dilute bubbles in the warm diffuse interstellar gas. Isotropy is violated, for example by gravity and large scale magnetic fields. The most important drivers of interstellar turbulence are stellar explosive events (supernova explosions and stellar winds), which strongly heat, accelerate and compress the ISM, driving shock waves (e.g. *Ostriker and McKee, 1988*). Other sources of turbulence include the Parker instability (*Parker,*

[1] Address: P.O. BOX 333, 90571 Oulu (mkorpi@moria.oulu.fi)

[2] Address: NE1 7RU, Newcastle upon Tyne (Axel.Brandenburg@newcastle.ac.uk)

[3] Address: P.O. BOX 333, 90571 Oulu (Ilkka.Tuominen@oulu.fi)

Studia geoph. et geod. 42 (1998), 410-418

1992), the Balbus-Hawley instability (*Balbus and Hawley, 1991*) and large scale shear stresses provided by galactic differential rotation (*Fleck, 1981*).

It is generally believed (e.g. *Beck et al., 1996; Zweibel and Heiles, 1997*) that the observed large scale magnetic fields in galaxies are generated by the action of a hydromagnetic dynamo (*Parker, 1955; Steenbeck, Krause & Rädler, 1966*). In contrast to the galactic rotation, the knowledge of interstellar turbulence is rather poor. However, there has recently been a lot of interest in calculating the mean-field transport coefficients (α and η_t) resulting from isolated supernova (hereafter SN) explosions occuring in magnetized, rotating and vertically stratified galactic discs (e.g. *Ferrière, 1996; Ziegler et al., 1996*). The resulting α-effect and turbulent diffusivity are weaker than expected, although in the model of *Ferrière (1996)* superbubbles, which are huge cavities produced by clustered SNe, were found to produce significantly larger values of the transport coefficients.

Due to the development of computer technology it is now possible, in addition to calculating the mean-field transport coefficients, to investigate the general properties of interstellar turbulence. Recent work on realistic models of the ISM has been done e.g. by *Rosen et al. (1995)*, who developed a global two-dimensional model of the ISM, and *Vázquez-Semadeni et al. (1996)*, who investigated the effects of cooling induced compressibility on turbulent flows in three dimensions. Our present work aims at investigating the general properties of SN driven interstellar turbulence using a local three-dimensional model of the warm and hot phases of the interstellar medium under Galactic conditions. The temperature of the cold phase is not correctly reproduced, but it is included in the sense that the scale height of the average density is only 100 pc, and not 500 pc, which is the scale height of the warm phase alone. In this paper we present results both for single SNe and multiple interacting SNe.

2. THE MODEL

We take a local Cartesian frame of reference where the x-direction points away from the Galactic centre, y in the azimuthal direction and z along the rotation axis. The centre of the box is moving on a circular orbit with radius R and angular velocity Ω_0 about the Galactic centre. We define a shear parameter $q = -\partial \ln \Omega / \partial \ln r$, where r is the distance from the rotation axis. In the solar neighbourhood $\Omega \propto r^{-1}$, which yields $q = 1$. In our local frame of reference the shear in angular velocity translates to a linear shear velocity $u_y^{(0)} = -q\Omega_0 x$ (*Wisdom and Tremaine, 1988*). In the following we solve for the deviations $\mathbf{u}$ from this basic flow. We solve the uncurled induction equation for the magnetic vector potential, the momentum equation, the energy equation and the continuity equation, which we can write in the following form:

$$\frac{\mathcal{D}\mathbf{A}}{\mathcal{D}t} = \mathbf{u} \times \mathbf{B} + q\Omega_0 A_y \hat{\mathbf{x}} - \eta\mu_0 \mathbf{J}, \tag{1}$$

$$\frac{\mathcal{D}\mathbf{u}}{\mathcal{D}t} = -\mathbf{u} \cdot \nabla \mathbf{u} + \mathbf{g} - \frac{1}{\rho}\nabla p + f(\mathbf{u}) + \frac{1}{\rho}\mathbf{J} \times \mathbf{B} + \frac{1}{\rho}\nabla \cdot \tau, \tag{2}$$

$$\frac{\mathcal{D}e}{\mathcal{D}t} = -\mathbf{u}\cdot\nabla e - \frac{p}{\rho}\nabla\cdot\mathbf{u} + \frac{1}{\rho}\nabla\cdot(\chi\rho\nabla e) + 2\nu\mathbf{S}^2 + \frac{\eta\mu_0}{\rho}\mathbf{J}^2 + \rho\Lambda + \Gamma, \tag{3}$$

$$\frac{\mathcal{D}\ln\rho}{\mathcal{D}t} = -\mathbf{u}\cdot\nabla\ln\rho - \nabla\cdot\mathbf{u}, \tag{4}$$

where the time derivative $\mathcal{D}/\mathcal{D}\ t = \partial/\partial t + u_y^{(0)}\partial/\partial y$ includes the transport by our basic flow. In equation (2) the term $f(\mathbf{u}) = \Omega_0(2u_y, -(2-q)u_x, 0)$ describes epicyclic deviations from the purely circular rotation, which arise from the Coriolis force $\mathbf{F}_C = -2\ \mathbf{\Omega}\times\mathbf{u}$ and part of the inertia force $-u_x du_y^{(0)}/dx = q\Omega_0 u_x$. The gravity in the vertical direction is assumed to be

$$\mathbf{g} = -\mathbf{z}\left(\frac{c_s}{H}\right)^2\left(1+\left(\frac{z}{H}\right)^2\right)^{-1/2}, \tag{5}$$

where c_s is the isothermal sound speed and H is the scale height of the disc. The loss term $\rho\Lambda$ in the energy equation describes the radiative cooling of the interstellar medium. The cooling function $\Lambda = \Lambda_i T^{\beta_i}, T_i \leq T < T_{i+1}$, is adopted from *Vázquez-Semadeni et al. (1996)*. Temperature T is measured in Kelvins and Λ in ergs^{-1} g^{-2} cm^3 (see Table 1). The energy source term describing the heating due to supernova explosions is

$$\Gamma = g(t)\frac{E_{SN}}{\rho V}, \tag{6}$$

where E_{SN} is the explosion energy, $V = \delta x\ \delta y\ \delta z$ is the explosion volume, $\delta x = \delta y = \delta z$ is our spatial resolution and $g(t) = 1$ when $t_1 \leq t \leq t_2$. We assume that supernovae are randomly distributed in the Galactic disc having an explosion rate σ per unit area. In the vertical direction the distribution is considered to be exponential with scale height H_{SN}, which yields the explosion rate per unit volume

$$\Sigma(z) = \frac{\sigma}{2H_{SN}}e^{-|z|/H_{SN}} \tag{7}$$

The remaining quantities have their usual meaning: $\mathbf{J} = \mu_0^{-1}\nabla\times\mathbf{B}$ is the current density, μ_0 the vacuum permeability, ν the kinematic viscosity, $\tau = 2\nu\rho\mathbf{S}$ the stress tensor, $S_{ij} = \frac{1}{2}\left(\partial_j u_i + \partial_i u_j, -\frac{2}{3}\delta_{ij}\partial_k u_k\right)$, η the magnetic diffusivity and χ the thermal diffusivity. We assume a perfect gas law $p = \rho e(\gamma-1)$ with $\gamma = c_p/c_v = 5/3$. The temperature is related to the internal energy by $e = c_v T$.

We assume stress-free, electrically insulating boundary conditions at the top and the bottom of the box (along the z-direction), i.e.

$$\frac{\partial u_x}{\partial z} = \frac{\partial u_y}{\partial z} = u_z = \frac{\partial e}{\partial z} = \frac{\partial A_x}{\partial z} = \frac{\partial A_y}{\partial z} = A_z = 0. \tag{8}$$

In the azimuthal (y) direction periodic boundary conditions are applied, and boundary conditions are quasi-periodic in the radial (x) direction accounting for the effect of the shear flow: $F(L_x, y, z) = F(0, y + q\Omega_0 L_x t, z)$, where F represents any of the eight dependent variables.

Equations (1)-(3) are solved numerically using a third-order *Hyman (1979)* scheme for the time stepping and a sixth-order compact scheme for the spatial derivatives (*Lele, 1992*). We adopt artificial viscosities to capture shocks and hyperviscous fluxes to stabilize advection and waves. The shock capturing viscosity is nonvanishing in the regions where $-\nabla \cdot \mathbf{u} > 0$ and proportional to $-\nabla \cdot \mathbf{u}$ there. The hyperviscosity is proportional to the modulus of the ratio of the third to the first derivative of the velocity field. A more detailed description of the code is given in *Brandenburg et al. (1995)*. The code was validated examining single nonradiative SN explosions, for which a simple analytical solution can be obtained using self-similarity arguments (*Sedov, 1959*). The density, temperature, pressure and velocit y profiles were found to be in agreement with the analytical solution.

We take a box of dimensions $L_x = L_y = L_z = 0.5$ kpc located at reference radius $R = 10$ kpc in the Galaxy. We use a numerical resolution of $81 \times 81 \times 81$ corresponding to $\delta x = \delta y = \delta z = 6.2$ pc. We take the angular velocity in the solar neighbourhood to be $\Omega_0 = 25$ km s^{-1} kpc^{-1}. We have an initially uniform internal energy $e = e_0$, where e_0 is determined by the isothermal sound speed $c_s = \sqrt{(\gamma - 1)\, e_0}$, which we set to be 10 km s^{-1}. We adopt hydrostatic equilibrium initially with

$$\rho = \rho_0 \, \exp\left(1 - \sqrt{1 + \left(\frac{z}{H}\right)^2}\right), \tag{9}$$

corresponding to the gravity adopted, Eq. (5), where $H = 100$ pc is the scale height of the Galactic disc and $\rho_0 = 2 \cdot 10^{-24}$ g cm^{-3} is the average density in the Galactic midplane. Initially we assume $\mathbf{u} = 0$. We apply uniform azimuthal magnetic field $\mathbf{B} = (0, \sin(\pi z / L_z), 0)$, whose strength is of the order of 1μG.

We use parameters describing type II SNe, because type I SNe have lower Galactic frequency and larger scale height and therefore contribute less to events in our computational domain. We take $H_{SN} = 90$ pc and $\sigma = 1.2 \cdot 10^{-5}$ kpc^{-2} yr^{-1}. These values give approximately one SN in every 330 000 years in the Galactic midplane. We consider explosions releasing the energy $E_{SN} = 10^{51}$ erg, which occur in a single gridpoint corresponding to the explosion volume $V = \delta x^3$.

Table 1. The cooling function used

T_i [K]	Λ_i [$erg\ s^{-1} g^{-2} cm^3$]	β_i
100	$1.14 \cdot 10^{15}$	2.000
2000	$5.08 \cdot 10^{16}$	1.500
8000	$2.35 \cdot 10^{11}$	2.867
10^5	$9.03 \cdot 10^{28}$	-0.650

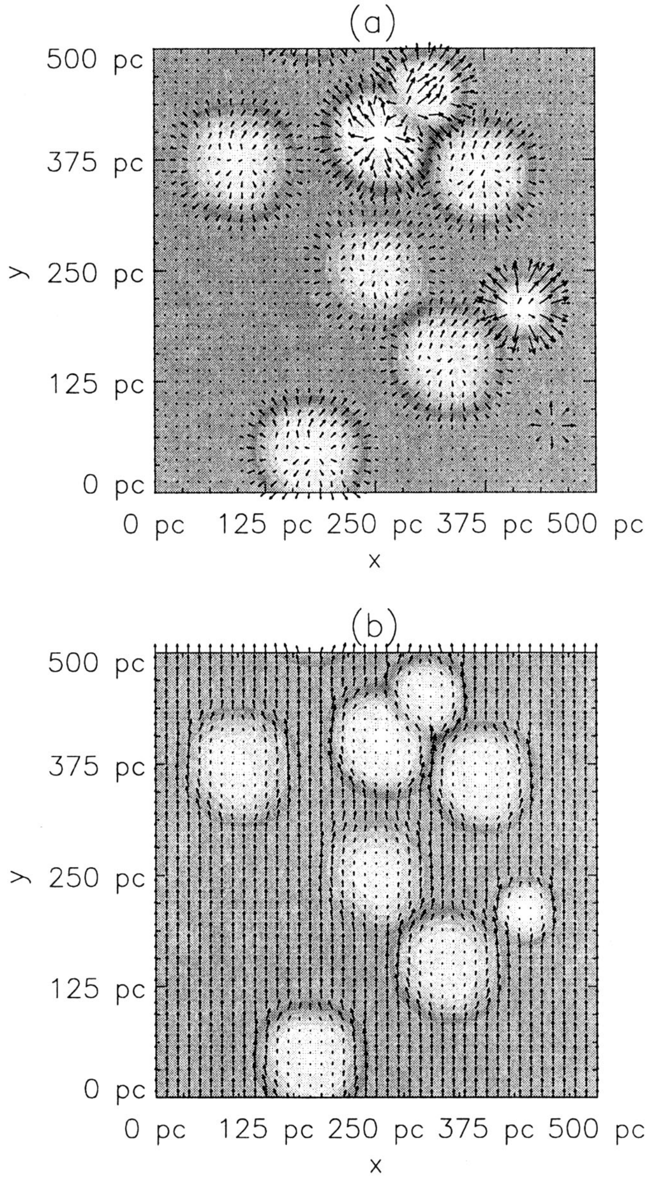

Fig. 1. Typical snapshot of a run with multiple SNe. These plots are xy-slices at the Galactic midplane. Panel (a) shows velocity field and panel (b) magnetic field superimposed on density contours at t=4.4 Myr. The scaling of the velocity field is logarithmic due to the large contrast between the velocities in young and old remnants. Darkest colour represents density $6 \cdot 10^{-24}$ g cm^{-3} and the lightest 10^{-27} g cm^{-3}. Maximum velocity in these plots is of order 300 km s^{-1} and maximum magnetic field strength is of order 2 μG.

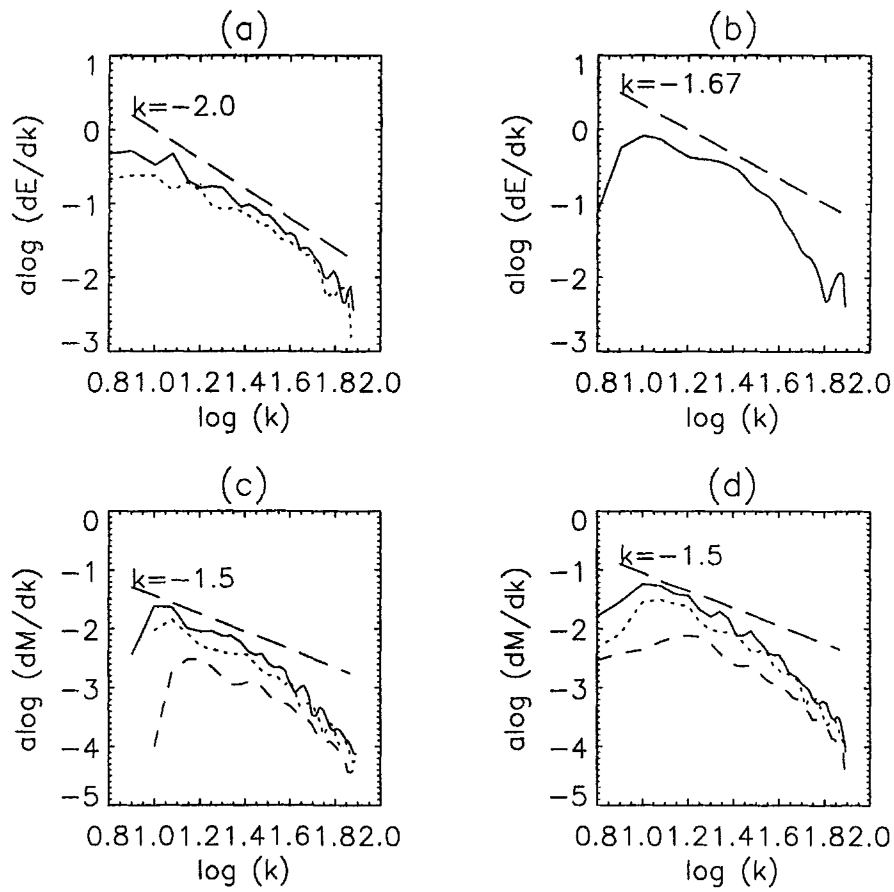

Fig. 2. Magnetic and kinetic energy spectra in a run with multiple SNe. In these plots the units of kinetic and magnetic energy are $[E_K] = [E_M] = 3 \cdot 10^{50}$ erg and the unit of wavenumber is $[k] = \mathrm{kpc}^{-1}$. In panel (a) the kinetic energy spectrum at $t = 1.4$ Myr (dotted) and $t = 3.0$ Myr (solid) is plotted. A spectrum with spectral index consistent with $k = -2$ is observed at both times. Panel (b) shows the kinetic energy spectrum at $t = 4.4$ Myr, when the spectral index is approximately $k = -5/3$. Panels (c) and (d) show magnetic energy spectrum at $t = 1.4$ Myr (dotted), $t = 3.0$ Myr (dashed) and $t = 4.4$ Myr (solid). In panel (c) spectra of radial and vertical components are plotted and panel (d) shows the spectra of the azimuthal component. At $t = 1.4$ Myr radial and vertical components are characterized by a spectrum close to $k = -1$, but later on they show spectrum with spectral index consistent with $k = -3/2$. During the early stages the azimuthal component of the magnetic field shows a spectrum with spectral index $k = -3/2$, but later on the slope gets steeper.

3. RESULTS

In our model SNe are modelled as instantaneous explosive events releasing large amounts (10^{51} ergs) of thermal energy. This thermal energy is efficiently converted to kinetic energy during the first 500 years of the supernova remnant's (hereafter SNR) evolution. During the free expansion phase, when the mass of the initial ejecta still exceeds the swept-up mass, expansion velocities up to 1200 km s^{-1} are present yielding a Mach number Ma$\approx$100, and a shock forms. Single SN remnant at the shock stage was found to produce a kinetic energy spectrum with spectral index $k = -2$ at scales 35–80 pc. The initially ubiquitous azimuthal magnetic field (1 μG) is expelled from the interior of the remnant, and radial and vertical magnetic fields are produced from the azimuthal one. The azimuthal magnetic field shows a power-law spectrum with spectral index close to $k = -3/2$, while the weaker radial and vertical components have a spectral index $k = -1$.

After 2 Myr the propagation velocity of the shock front drops below the ambient sound speed and the shock dies out. There is still a cool dense shell with a hot interior left from the SN explosion. During this dense shell stage Coriolis force and large-scale shear due to Galactic rotation become significant, because the diameter of the remnant is larger. Large-scale shear stretches the remnant and it becomes elliptically shaped. Radial expansion gives rise to Coriolis force, which generates a tangential velocity component and causes the remnant to counterrotate as a whole. These processes, and possibly also thermal instability for $T > 10^5$ K due to the properties of our cooling function (cf. Table 1), produce some small scale motions inside the remnant. Vorticity production, however, was found to be weak.

When we allow for multiple SNe there are both young SNe driving shock waves and older remnants at the dense shell stage, and also SN interactions are possible. In Fig. 1a,b a typical snapshot of a run with multiple SNe is presented showing SNe at different evolutionary stages. During the first 3 Myr, when there are equal amounts of shock fronts and dense shells, but no supernova interactions, kinetic shock spectrum with spectral index $k = -2$ is observed (see Fig. 2a), which indicates that the vorticity production due to Galactic rotation and Coriolis force acting on the older remnants is less important. The observed shock spectrum is wider than in the case of single SN (20–125 pc) because there are remnants of different sizes. The more important role of older remnants is to produce density fluctuations in the interstellar medium. They produce "clumps", where the density contrast ρ_{max}/ρ_{min} between the cool dense shell and the interior can be 800 or even more. When young SNe having large amounts of kinetic energy collide with these older remnants, the propagation velocity of the shock front changes due to the changing density, and vortical motions are generated. When both of the colliding remnants are very energetic, reflections are also possible (see Fig. 1a), but their effect is essentially the same. These interactions occur often after 3 Myr, and after 4.4 Myr kinetic energy with spectral index $k = -5/3$ is observed indicating that the vortical motions have become dominant (see Fig. 2b). In the regions where supernova interactions occur the degree of magnetic field compression is higher and generation of radial and vertical magnetic field is enhanced. Instead of having spectral index $k = -1$, like in the isolation stage ($t = 1.4$ Myr), a spectrum with $k = -3/2$ is observed after 4.4 Myr (see Fig. 2c).

4. CONCLUSIONS

In the present paper we have investigated some general properties of SN driven interstellar turbulence. For single SN explosions we found that there are two major stages governing the evolution of a SN: a shock stage, when a shock spectrum is observed, and a dense shell stage, when Galactic rotation and Coriolis force act on the remnant. We also allowed for multiple SNe distributed randomly in the Galactic plane but exponentially in the vertical direction. At $t = 3.0$ Myr, when there were equal amounts of SNe at the shock and dense shell stage and no SN interactions, we observed a wide shock spectrum in the kinetic energy. This indicates that the vorticity production via Galactic rotation and Coriolis force is weak compared to shock production. SN interactions, however, were found to significantly amplify the vortex mode.

We have not made any experimentations with different SN parameters (σ, H_{SN}), which are especially important in determining the frequency of supernova interactions. Furthermore we did not include type I SNe because of their lower Galactic frequency and larger H_{SN}. Because of the density stratification, matter and magnetic fields tend to escape to the halo due to type II SN explosions. Therefore the role of type I SNe, occurring at higher latitudes, might be very important causing downward motions to compensate the escape of matter and magnetic fields. Another interesting question, which is also beyond the scope of this paper, is whether this kind of flow is capable of dynamo action or not. In future work we will try to answer these questions.

Acknowledgements: We thank Anvar Shukurov and Javier Sanchez-Salcedo for fruitful discussions and suggestions. This work was supported by the EC Human Capital and Mobility Networks project "Late type stars: activity, magnetism, turbulence" No. ERBCHRXCT940483

Manuscript received: 13th November, 1997; *Revisions accepted: 12th May, 1998*

References

Balbus, S. A. and Hawley, J. F., 1991: A powerful local shear instability in weakly magnetized disks. I - Linear analysis. II - Nonlinear evolution. *Astrophys. Journal*, **376**, 214-233

Beck, R., Brandenburg, A., Moss, D., Shukurov, A. and Sokoloff, D., 1996: Galactic magnetism: Recent developments and perspectives. *Annu. Rev. Astron. Astrophys.*, **34**, 155-206

Brandenburg, A., Nordlund, Å., Stein, R. F. and Torkelsson, U., 1995: Dynamo-generated turbulence and large-scale magnetic fields in a Keplerian shear flow. *Astrophys. Journal*, **446**, 741-754

Ferrière, K., 1996: Alpha-tensor and diffusivity tensor due to supernovae and superbubbles in the Galactic disk near the Sun. *Astron. Astrophys.*, **310**, 438-455

Fleck, R. C., 1981: On the generation and maintenance of turbulence in the interstellar medium. *Astrophys. Journal*, **246**, L151-L154

Hyman, J. M., 1979: A Method of Lines Approach to the Numerical Solution of Conservation Laws, In: *Adv. of Computation Methods for Partial Differential Equations, Vol III*, Publ. IMACS (ed. R. Vichnevetsky & R. S. Stepleman), pp. 313-343

Lele, S. K., 1992: Compact finite difference schemes with spectral-like resolution. *J. Comput. Phys.*, **103**, 16-42

Ostriker, J. P. and McKee, C. F., 1988: Astrophysical blastwaves. *Rev. Mod. Phys.*, **60**, 1-68

Parker, E. N., 1955: Hydromagnetic dynamo models. *Astrophys. Journal*, **122**, 293-314

Parker, E. N., 1992: Fast dynamos, cosmic rays and the galactic magnetic field. *Astrophys. Journal*, **401**, 137-145

Rosen, A. and Bregman, J. N., 1995: Global models of the interstellar medium in disk galaxies. *Astrophys. Journal*, **440**, 634-663

Sedov L. I., 1959, In: *Similarity and Dimensional Methods in Mechanics*, Infosearch Ltd., London

Steenbeck, M., Krause, F. and Rädler, K.-H., 1966: On the dynamo theory of stellar and planetray magnetic fields, I. A. C. dynamos of solar type. *Astron. Nachr.*, **291**, 49-84, [English translation: Roberts and Stix (1971) pp. 147-220]

Vázquez-Semadeni, E., Passot, T. and Pouquet, A., 1996: Influence of cooling-induced compressibility on the structure of turbulent flows and gravitational collapse. *Astrophys. Journal*, **473**, 881-893

Wisdom, J. and Tremaine, S., 1988: Local simulations of planetary rings. *Astron. Journal*, **95**, 925-940

Ziegler, U., Yorke, H. W. and Kaisig, M., 1996: The role of supernovae for the galactic dynamo I. The full alpha-tensor for uncorrelated explosions. *Astron. Astrophys.*, **305**, 114-124

Zweibel, E. G. and Heiles, C., 1997: Magnetic fields in galaxies and beyond. *Nature*, **385**, 131-136